Open Access Library Journal
2025, Volume 12, e14165
ISSN Online: 2333-9721
ISSN Print: 2333-9705

Contribution to Study and Mapping Landslide Hazard in the West Cameroon Region: Case of Double Landslide on Foréké Escarpment

Marie Roumy Ouafo[1*], Onana Ntouda[2], Amos Mogo[3], Olivier Leumbe[3]

[1]Department of Earth Sciences, Faculty of Science, University of Douala, Douala, Cameroon
[2]Research Branch, Natural Hazards Research Laboratory, National Institute of Cartography, Yaoundé, Cameroon
[3]Research Branch, Agricultural Research Institute for Development, Yaoundé, Cameroon
Email: *ouafoleumberoumy@gmail.com

How to cite this paper: Ouafo, M.R., Ntouda, O., Mogo, A. and Leumbe, O. (2025) Contribution to Study and Mapping Landslide Hazard in the West Cameroon Region: Case of Double Landslide on Foréké Escarpment. *Open Access Library Journal*, **12**: e14165.
https://doi.org/10.4236/oalib.1114165

Received: August 26, 2025
Accepted: November 30, 2025
Published: December 3, 2025

Abstract

With nearly 1.3 billion people living in mountainous regions worldwide, exposure to landslide risks is very high. Cameroon, with its morphological, climatic and soil diversity, is the site of frequent landslides. With climate change, the frequency and intensity of these disasters have increased significantly, and they now represent a threat to the lives and livelihoods of people in the western highlands. Over the past five years, the West Cameroon region has experienced two major landslides. The study produces a regional landslide hazard map for West Cameroon using an AHP-based GIS approach and Landsat land-use data. Four topographic factors extracted from SRTM DEMs are weighted with Saaty's method to build the hazard layer. The resulting hazard map shows 10.7% of the region in a high-risk class. A field case study of the 5 November 2024 double landslide on the Foréké escarpment links creep on a 56˚ slope, clay-rich soils, and road construction. Basic mitigation ideas (rainfall monitoring, slope stabilization) are proposed.

Subject Areas

Natural Hazard

Keywords

Western Highlands, Landslide, Slope, Creep, Mapping

1. Introduction

Landslide is a major disaster [1] [2] causing over 10,000 deaths worldwide every

year [3]. They can be very violent, as in Honduras in 1973 (2,800 deaths), Nepal in 2015 (400 deaths) or India in 2024 (413 deaths) [4] [5]. Because of their unpredictability [6], speed and brutality [7], they represent a great danger for populations and infrastructures [8]. In 2024, more than 400 landslides were recorded worldwide, and this is the highest number ever recorded in a single year [4]. Their intensification and increasing impact on populations are attributed to human pressure on territories sensitive to climate change [9]. Landslides, particularly active in mountain areas [10]-[13], can occur suddenly or more slowly over long periods [14] [15]. In Cameroon, they occur frequently in the western highlands (1978 at Dschang and Fossong Wentcheng, 1986 at Melong, 1991 at Pinyin, 1992 at Santa, 1993 at Bafaka, 2000 at Nwa, 2001 and 2009 in Limbe, 2002 in Bana, 2003 in Magha'a in Bafou and Wabane, 2005 in Fongo-Tongo, 2007 in Abuh and Kékem, 2008 in Santchou and Fondenera, 2011 in Kékem and Koutaba, 2019 in Bafoussam...etc.) [16]. The most recent is a double landslide of November 05, 2024, on the Foréké escarpment (more than 20 dead), which buried intercity transport vehicles, trucks and excavators. Unlike landslides recorded generally during the rainy season in Cameroon [11] [13] [14] [17]-[19], the November 05, 2024 case occurred during the dry season. The combination of natural and anthropogenic constraints led to a landslide by creep. As the conditions that prevailed at the end of the first landslide persist after the second, further landslides can occur on the site. Mitigating the impact requires a comprehensive analysis of the phenomenon [20] and a good understanding of spatio-temporal patterns [21] [22]. However, the complex nature of mechanisms behind landslides makes it difficult to grasp the prerequisites [23]. In a bid to reduce natural hazards on its territory, Cameroon has been pursuing a natural hazard prevention policy for several years now. Among the means developed, the mapping of risk zones is a fundamental tool. In order to reduce natural hazards on its territory, Cameroon has been implementing a natural hazard prevention policy for several years now. Among the means developed, the mapping of risk zones is a fundamental tool. Landslide-hazard maps are an essential tool for assessing landslide risk and contributing to public safety worldwide [24]. Natural risk is the combination of natural hazard and vulnerability. Natural hazard assessment consists of determining the spatial probability of occurrence of the phenomenon [25]. However, quantifying the hazard is intrinsically difficult because natural environmental conditions are uncertain and complex, so previous landslides are essential for refining assessment and validating the results. Although the various methods benefit from an increase in calculation capacity, they remain based on the relationship between previous landslides and the environmental factors of the site studied [22]. In order to validate the model, we mapped the landslide hazard on the Foréké escarpment and extended it to the West Cameroon region to create a prediction map. This map was then compared with the landslide distribution of the later period. Finally, measures to mitigate this disaster in the West Highlands are proposed.

2. Description of the Study Area

The Western region of Cameroon covers an area of 13,892 km^2. It lies between 4˚45' and 6˚10' north latitude and between 9˚50' and 11˚10' east longitude (**Figure 1**). Morphologically, it is made up of plateaus bordered by volcanic massifs, the highest of which (Mount Bambouto) reaches an altitude of 2740 m [17]. This massif is bordered to the south-west by the Mbo plain and the Nkam valley, and to the north-east by the Tikar plain and the Mbam valley. The Foréké escarpment forms the boundary with the Mbo plain. The equatorial climate (dry season from November to mid-March, rainy season from March to October) has a number of specific features depending on the geomorphology [26]. On the mountains and escarpments, the climate is very cool and permanently foggy, with very low temperatures (10˚C to 15˚C on average) and high rainfall (over 2500 mm per year) [27]. On the plateau, the climate is cool and humid, with an average monthly temperature of around 18˚C and average annual rainfall of 1690 mm [28]. On the

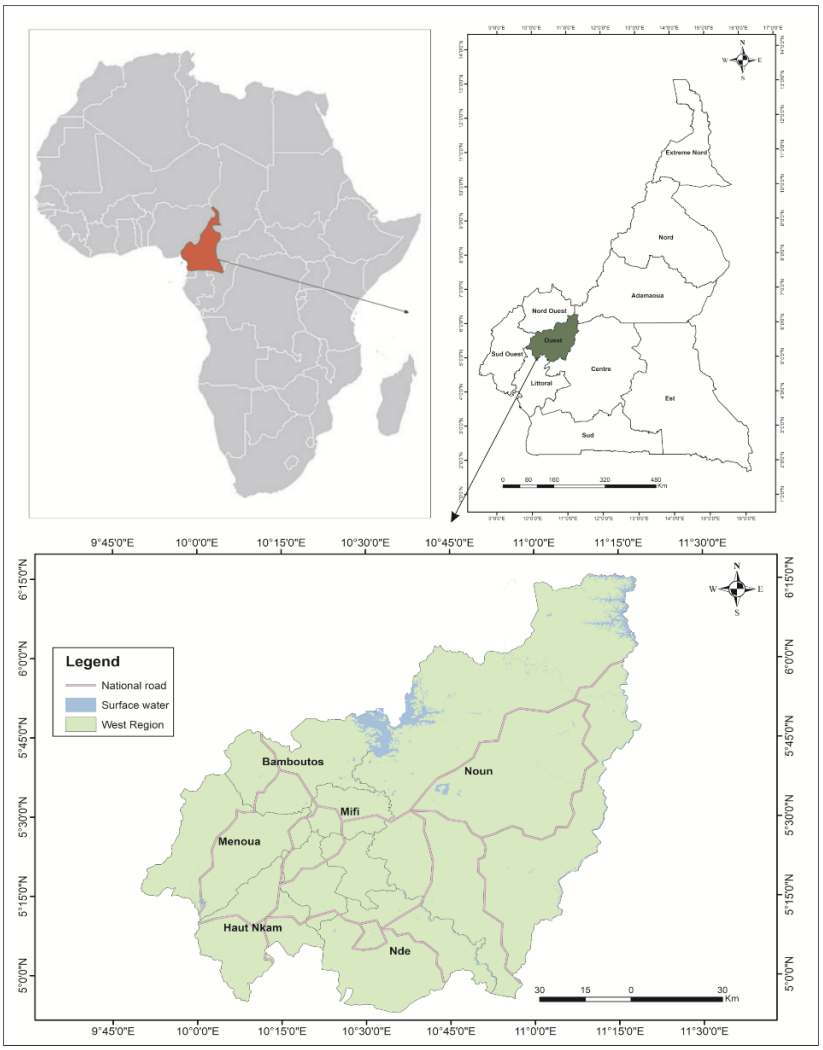

Figure 1. Location map of the study area. (Source: ArcGIS 10.8 (ESRI) software, from the topographic base sheets of Cameroon produced by the National Institute of Cartography)

plain, the average annual rainfall is 1750 mm and the average monthly temperature is 23.5˚C [29]. Phytogeographically, the region is composed of grassland at the summit [28], a shrub stratum and dense grass stratum on the plateau [30] and raffia trees in the valley [27]. The hydrographic network is dense, with falls and rapids cutting rivers at escarpments [31]. Geologically, rhyolites, trachytes and basalts rest on a granitic bedrock [17] [32] [33]. Andosols are found in the mountains, red ferric soils on the plateaus and ferruginous soils on the plains [11] [34] [35] [36].

3. Methods

The hazard map was produced using the Saaty method. Topographical features are derived from the Shuttle Radar Topography Mission (SRTM) digital terrain model, based on data from the National Geospatial-Intelligence Agency (NGA) and the National Aeronautics and Space Administration (NASA). Using ArcGIS 10.3 software, layers (slope, profile of curvature, terrain ruggedness index and altitude above the channel) were produced. These layers were weighted according to Saaty's task importance scale (**Tables 1-8**). The hazard maps were produced using a 12.5 m resolution DTM. Data pre-processing began with the representation of the hydrographic network on the DTM. The data were then processed successively.

For the generation of the layers, the following procedures have been followed in SagaGIS 7.2:

Slope: "Terrain Analysist"—"Morphometry"—"Slope"—"Aspect"—"Curvature".

Profile of curvature: both are generated in the "Geoprocessing", "Terrain Analyst", and "Basic Terrain Elements".

Terrain ruggedness index: "Terrain Analysist"—"Hydrology"—"Topographic Wetness index".

Altitude above the channel: "Terrain Analyst", "Preprocessing" and "Burn stream".

Modelling was carried out with the software ArcGIS, using the "Raster Calculator" tool—"Map algebra".

3.1. Weights Assignments

Table 1. Weight assignment.

Expression	Numeric value	Explanation
Equal importance	1	Both activities contribute equally to the objective
Moderate importance	3	Experience and judgment favor one activity over the other
High importance	5	Experience and judgment strongly factor one activity over the other
Very high importance	7	One activity is strongly favored and its dominance is demonstrated in practice

Continued

Extreme or absolute importance	9	Evidence favoring one activity over the other is of the highest possible order of affirmation
Intermediate degree of importance	2; 4; 6; 8	When a compromise between two expressions is required
Reciprocal importance	1/2; 1/3; 1/4; 1/5; …; 1/9	The reciprocal of the first 5 degrees

Table 2. Saaty weighted task importance scale.

Preference intensity	Associated value
Equal importance of both factors	1
One factor is moderately more important than the other	3
One factor is more important than the other	5
One factor is more important than the other	7
One factor has absolute importance over the other	9
Slightly less preference for the first factor than the second	1/3
Prefer the first factor less than the second	1/5
We much prefer the second factor to the first	1/7
The first factor is much less preferred than the second	1/9

Table 3. Binary comparison matrix.

	Slope	Profile of curvature	Terrain ruggedness index	Altitude above the channel
Slope	1	2	3	4
Profile of curvature	1/2	1	3	4
Terrain ruggedness index	1/3	1/3	1	2
Altitude above the channel	1/4	1/4	1/2	1
Columns sum	2.0833	3.05833	7.5	11

The binary comparison matrix is a preferential intensity assignment (Table 2) of two parameters. This pair-by-pair comparison of layers is assigned an associated value showing the importance of the layer in relation to the other on the outcome of the phenomenon.

The elements of the judgment matrix are obtained by dividing the value of each cell (Table 3) by the sum of the values corresponding to the column of that cell.

To obtain the weights of the factors, the sum per line (Table 4) corresponding to each factor was divided by the total sum of the lines.

The consistency of judgments was assessed by multiplying the associated value of the binary comparison matrix (Table 3) column by the weight of the

corresponding factor.

Consistency was calculated by dividing each sum of the rows in the judgement consistency score (Table 6) by the weight corresponding to the criterion.

Table 4. Result of judgment matrix.

	Slope	Profile of curvature	Terrain ruggedness index	Altitude above the channel	Lines sum
Slope	0.4800	0.5581	0.4	0.3636	1.8017
Profile of curvature	0.2400	0.2791	0.4	0.3636	1.2827
Terrain ruggedness index	0.1600	0.0930	0.1333	0.1818	0.5681
Altitude above the channel	0.1200	0.0697	0.0666	0.0909	0.3472
Total lines sum					3.9997

Table 5. Results of factor weights.

Factor	Slope	Profile of curvature	Terrain ruggedness index	Altitude above the channel
Weight	0.4505	0.3207	0.1420	0.0868
Weight in %	45.05	32.07	14.20	8.68

Table 6. Results of the assessment consistency of judgments.

	Slope	Profile of curvature	Terrain ruggedness index	Altitude above the channel	Lines sum
Slope	0.4505	0.6414	0.426	0.3472	1.8651
Profile of curvature	0.2252	0.3207	0.426	0.3472	1.3191
Terrain ruggedness index	0.1502	0.1069	0.1420	0.1736	0.5727
Altitude above the channel	0.1126	0.0802	0.071	0.0868	0.3506

Table 7. Consistence.

Factor	Slope	Profile of curvature	Terrain ruggedness index	Altitude above the channel
Consistency	4.1401	4.1132	4.0331	4.0391

Table 8. Random index.

N	1	2	3	4	5	6	7	8	9	10	11	12	13	14	15
IA	0	0	0.58	0.90	1.12	1.24	1.32	1.41	1.45	1.49	1.51	1.48	1.56	1.57	1.59

Consistency was calculated by dividing each sum of the rows in the judgement consistency score (Table 6) by the weight corresponding to the criterion.

We can then determine:

$$\gamma_{\max} = \frac{\sum Consistency}{6} = 4.0814$$

$$IC = \frac{\gamma_{max-n}}{n-1} = 0.0271$$

$$RC = \frac{IC}{IA} = 0.0301$$

With: γ_{max} : max value for 4 criteria; *n*: number of factors; *IC:* consistency index; *IA:* random index linked to the number of factors; *RC*: consistency ratio.

The matrix is sufficiently coherent as RC < 0.1

3.2. Field Work and Laboratory Analysis

A soil pit was dug manually, a profile described and soil samples collected. The horizon's thickness was measured with a tape, and the colour was determined using the Munsell soil colour chart. Samples are collected and stored in plastic bags previously labelled. Accessible past landslides were described, and geographical coordinates were recorded using Garmin 73 GPS navigation devices. Morphometric measurements were also taken using a double decameter and a clinometer. In the laboratory, granulometry was carried out using the Robinson pipette method after dispersion with sodium hexametaphosphate.

The analysis results are presented in Table 9.

Table 9. Physical characteristics of Foréké soils.

Depth	0 - 20 cm	30 - 40 cm	60 - 80 cm	90 - 135 cm
Sand	17.31	32.34	31.15	20.6
Silt	31.96	17.96	13.35	14.6
Clay	50.73	49.70	56.50	64.8

4. Results

4.1. Characterization of Foréké Soils

The profile made in the Foréké village shows from top to bottom:

0 - 20 cm: A dark-brown humus horizon (10YR4/3), clay-loam, friable, plastic, lumpy structure and dense root.

200 - 135 cm: A reddish-brown horizon (7.5YR5/6), clayey, porous, plastic, coarse polyhedral structure.

135 - 530 cm: Red alloterite (2.5R3/8), silty-clayey, porous, small weakly indurated rock fragments representing about 30% of the horizon.

530 - 750 cm: Silty isalterite with juxtaposition of yellowish (2.5Y5/3), reddish (5R3/6) and whitish-gray (10YR8/3) domains, presence of rock fragments.

750 to more than 1200 cm: Whitish-grey isalterite (10YR8/3), sandy-loamy, quartz grains up 40% of the horizon, many rock fragments.

4.2. Landslide Hazard Mapping along the Foréké Escarpment

4.2.1. Characterization of the Double Landslide on the Foréké Escarpment

The double landslide of November 05, 2024, is a major landslide that occurred at the "Nteh-Gwang" steep hill (56˚). The crater is subcircular, with a diameter of over 70 m and a depth of 40 m. Around 130,000 m^3 of material was mobilized, and the toe is over 350 m (Figure 2 and Figure 3).

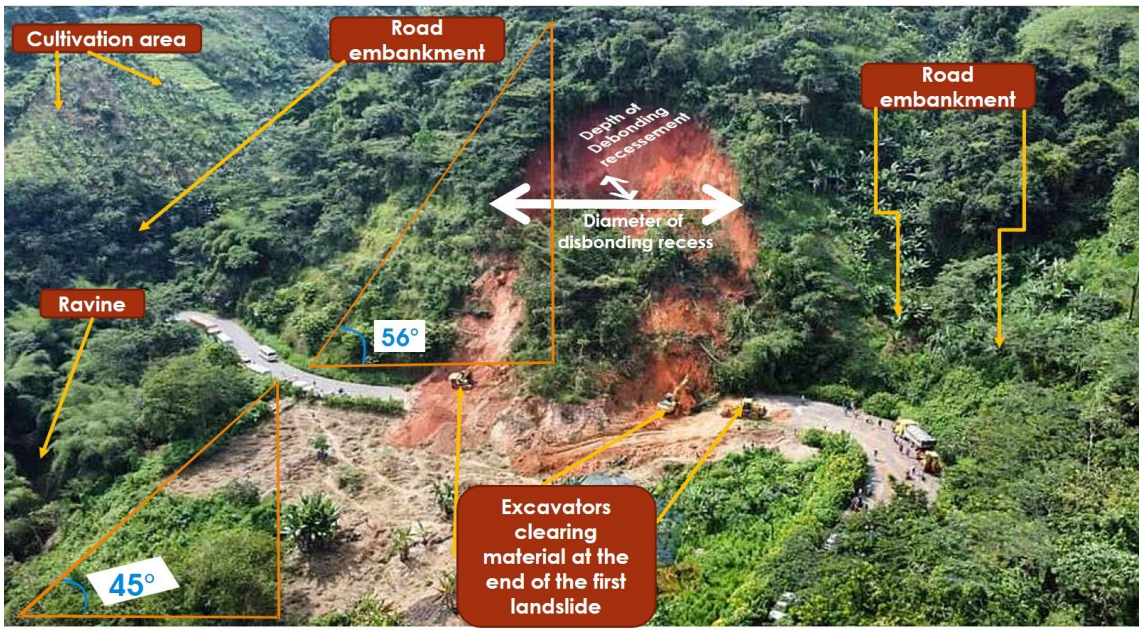

Figure 2. Characteristics of the first landslide.

Figure 3. Starting of the second landslide.

4.2.2. Landslide Hazard along the Dschang_Santchou Road

The slope inclination on the site of November 05, 2024, double landslide reaches 296% (Figure 4(a)), the profile of curvature reaches +0.03 (Figure 4(b)),

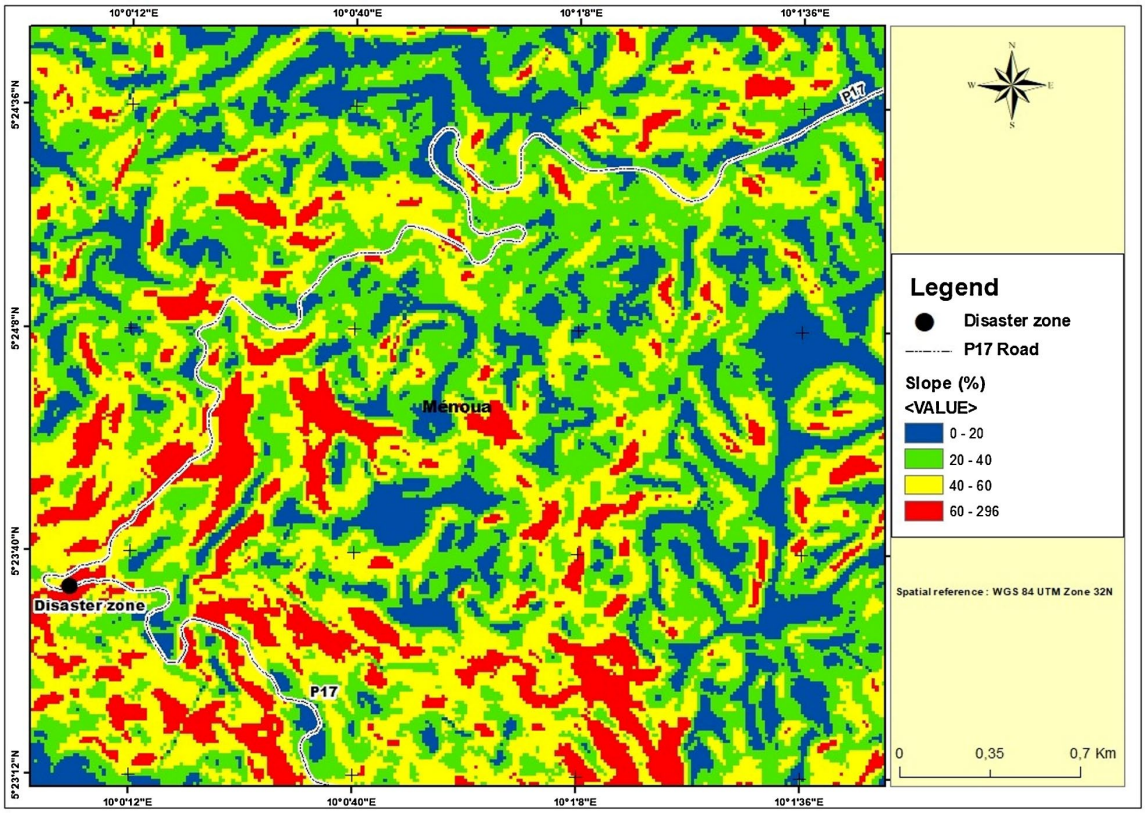
10°0'12"E
10°0'40"E
10°1'8"E
10°1'36"E
5°24'36"N
5°24'8"N
5°23'40"N
5°23'12"N
P17
Ménoua
Disaster zone
P17
Legend
Disaster zone
P17 Road
Slope (%)
<VALUE>
0 - 20
20 - 40
40 - 60
60 - 296
Spatial reference : WGS 84 UTM Zone 32N
0
0,35
0,7 Km

(a)

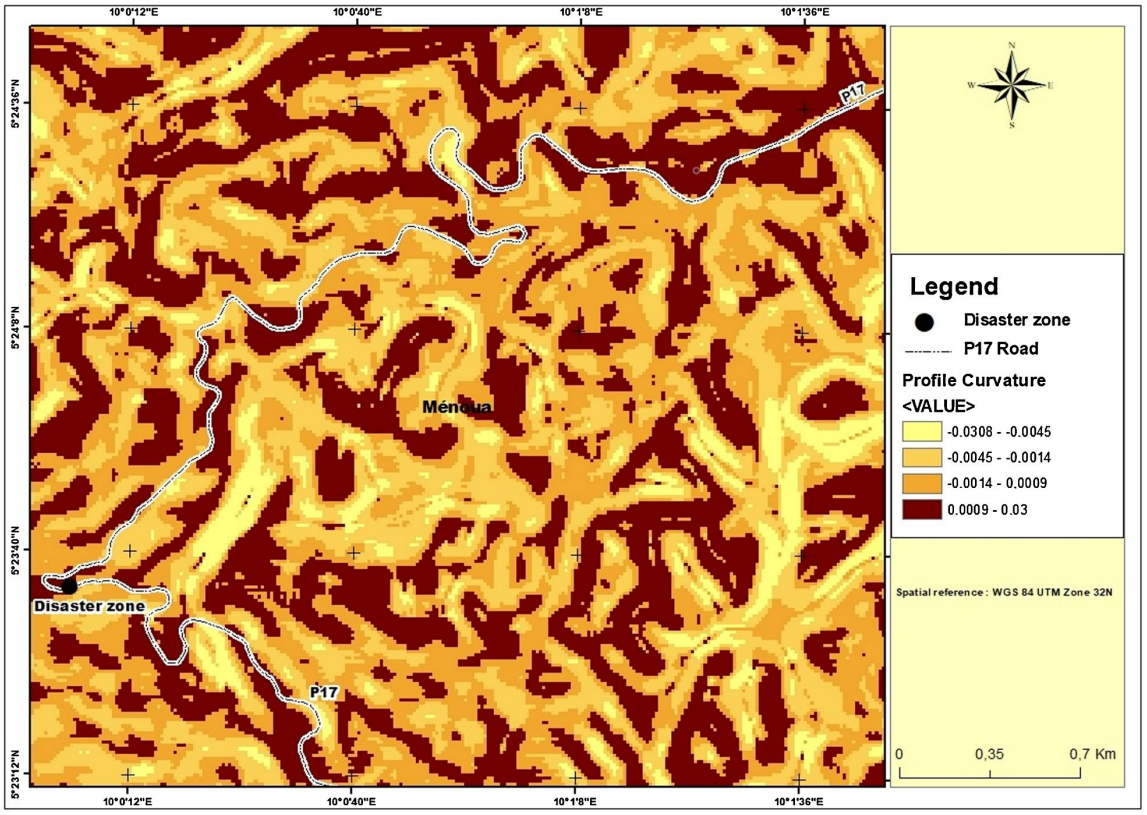
10°0'12"E
10°0'40"E
10°1'8"E
10°1'36"E
5°24'36"N
5°24'8"N
5°23'40"N
5°23'12"N
P17
Ménoua
Disaster zone
P17
Legend
Disaster zone
P17 Road
Profile Curvature
<VALUE>
-0.0308 - -0.0045
-0.0045 - -0.0014
-0.0014 - 0.0009
0.0009 - 0.03
Spatial reference : WGS 84 UTM Zone 32N
0
0,35
0,7 Km

(b)

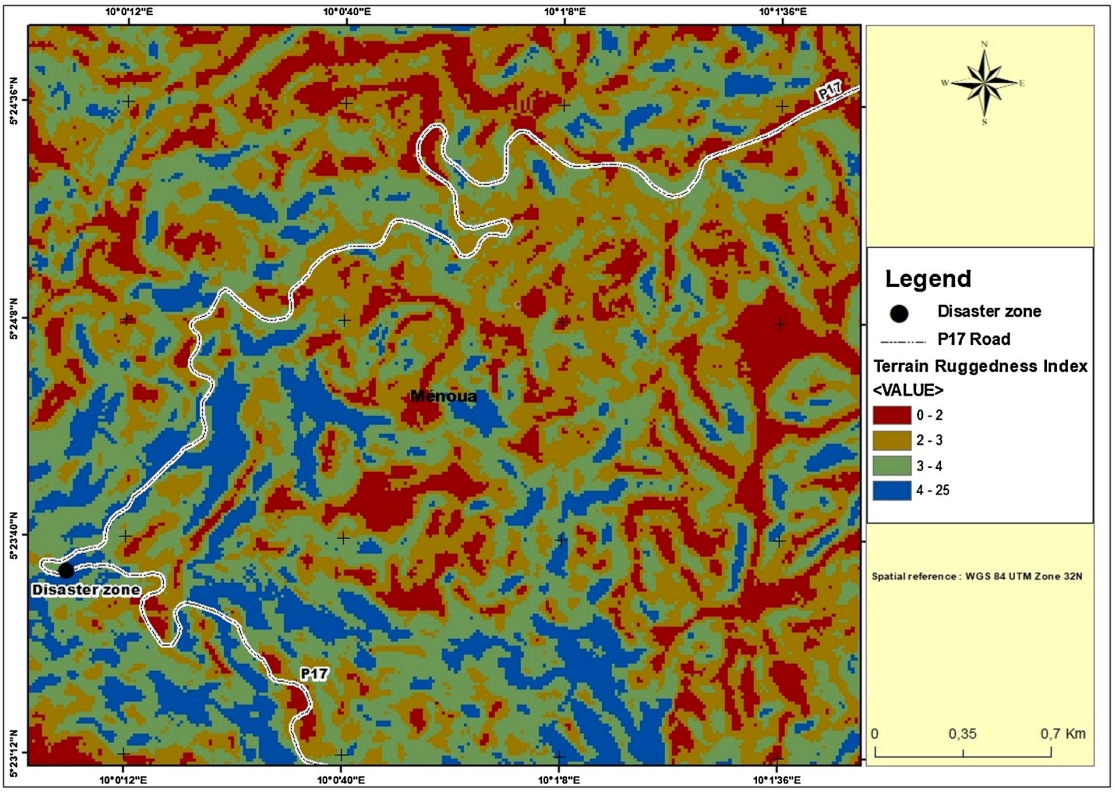

(c)

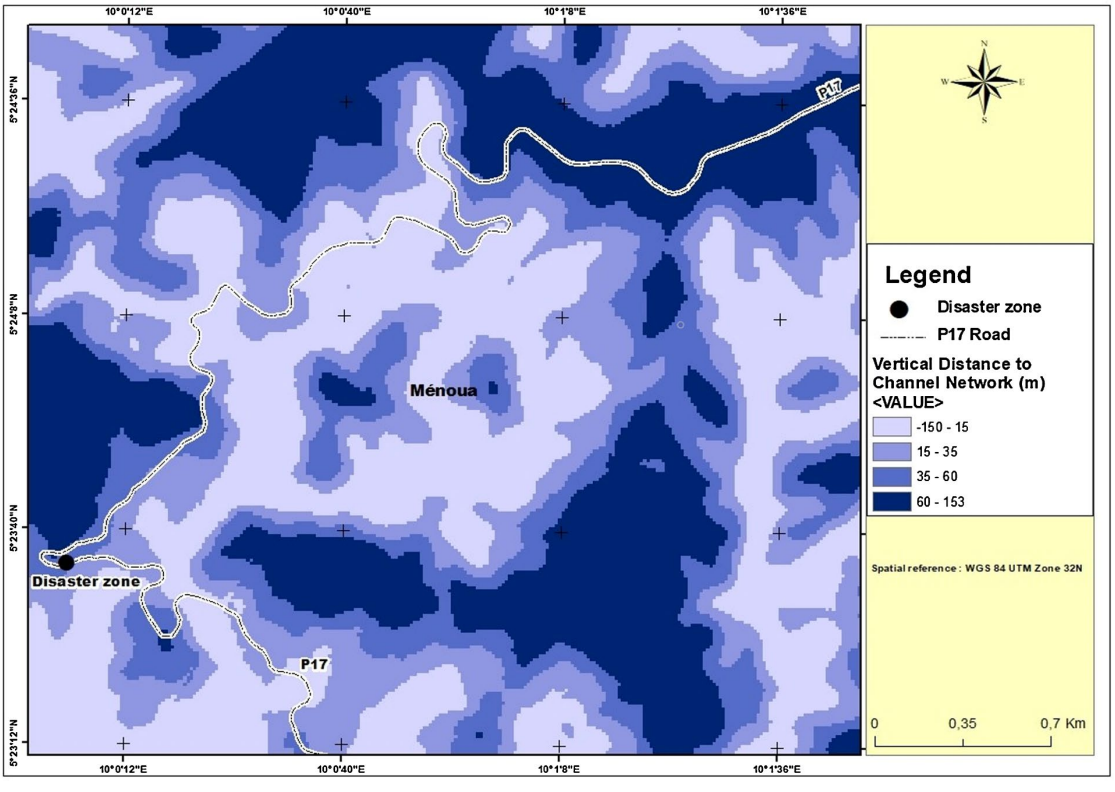

(d)

Figure 4. (a) Slope; (b) Profile of curvature; (c) Terrain ruggedness; (d) Terrain ruggedness.

the terrain ruggedness index reaches 25 (Figure 4(c)) and the altitude above the channel reaches +153 m (Figure 4(d)). The Ménoua River, the main collector in the study area, is located at 1031 m from the "Nteh-Gwang" hill. About 35% of the Dschang_Santchou road presents a high hazard (Figure 5).

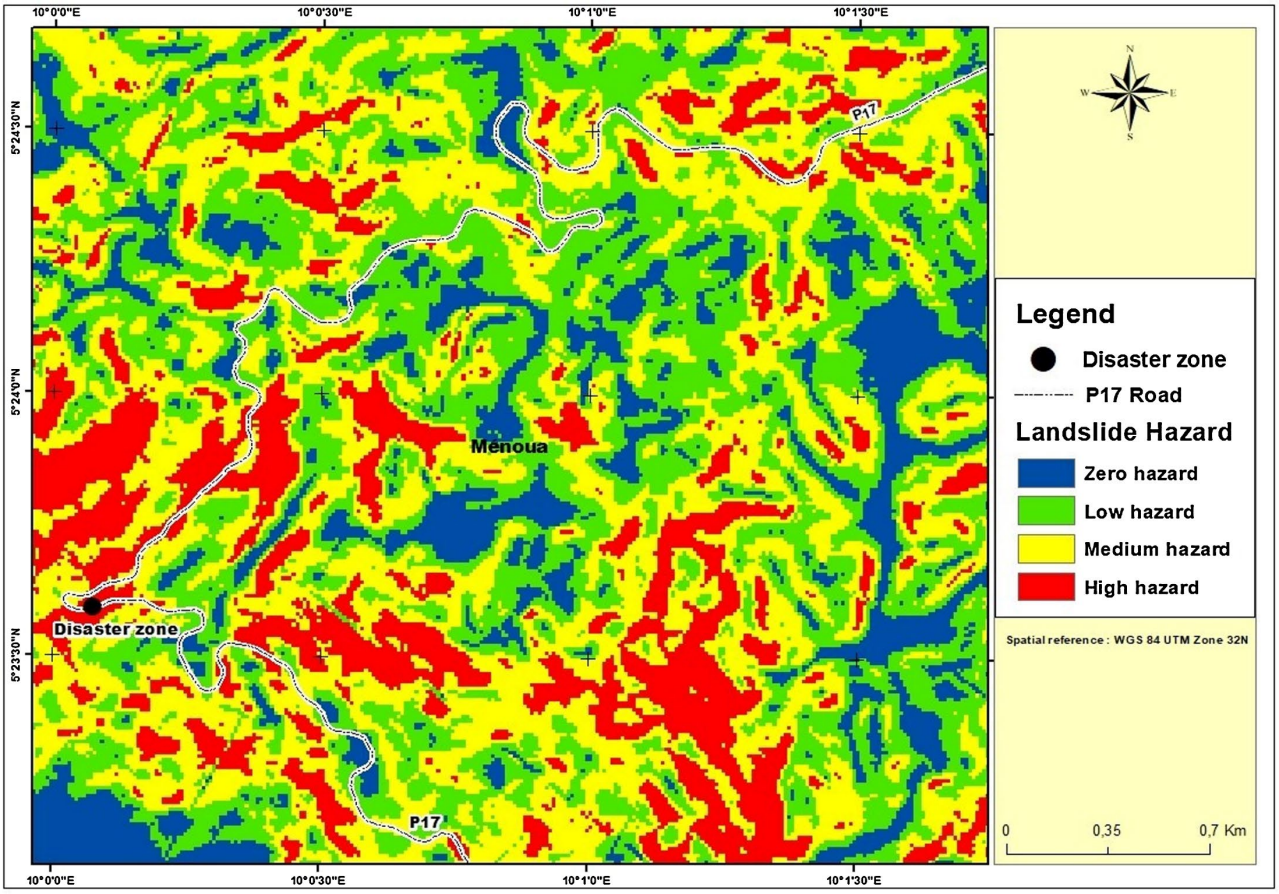

Figure 5. Risk map along the Foréké escarpement. (Source: ArcGIS 10.8 (ESRI) software, from the topographic base sheets of Cameroon produced by the National Institute of Cartography)

4.3. Landslide Hazard Mapping in West Cameroon Region

In the West Cameroon region, the slope inclination varies from 0 to 692% with a maximum along the escarpments bordering the highlands (Figure 6(a)). The profile of curvature varies from −0.09 to +0.08, with the minimum value on the Bambouto volcanic massif (Figure 6(b)). The terrain ruggedness index varies from 0 to 64, with a maximum along the escarpments bordering the highlands (Figure 6(c)). The altitude above the channel varies from −275 to +891 m with a maximum along the escarpments bordering the highlands (Figure 6(d)). High-hazard zones represent 6.40% of the Western Region, medium-hazard zones 8.47% and low-hazard zones 25.14% (Figure 7). High-hazard zones are located in the highlands (between 1200 and 1800 m).

All control cases (Ngouache, Magha'a, Fongo-Tongo, Dschang, Fossong-Wentche, Santchou, Kekem) are located perfectly in high-hazard zones (Figure 8).

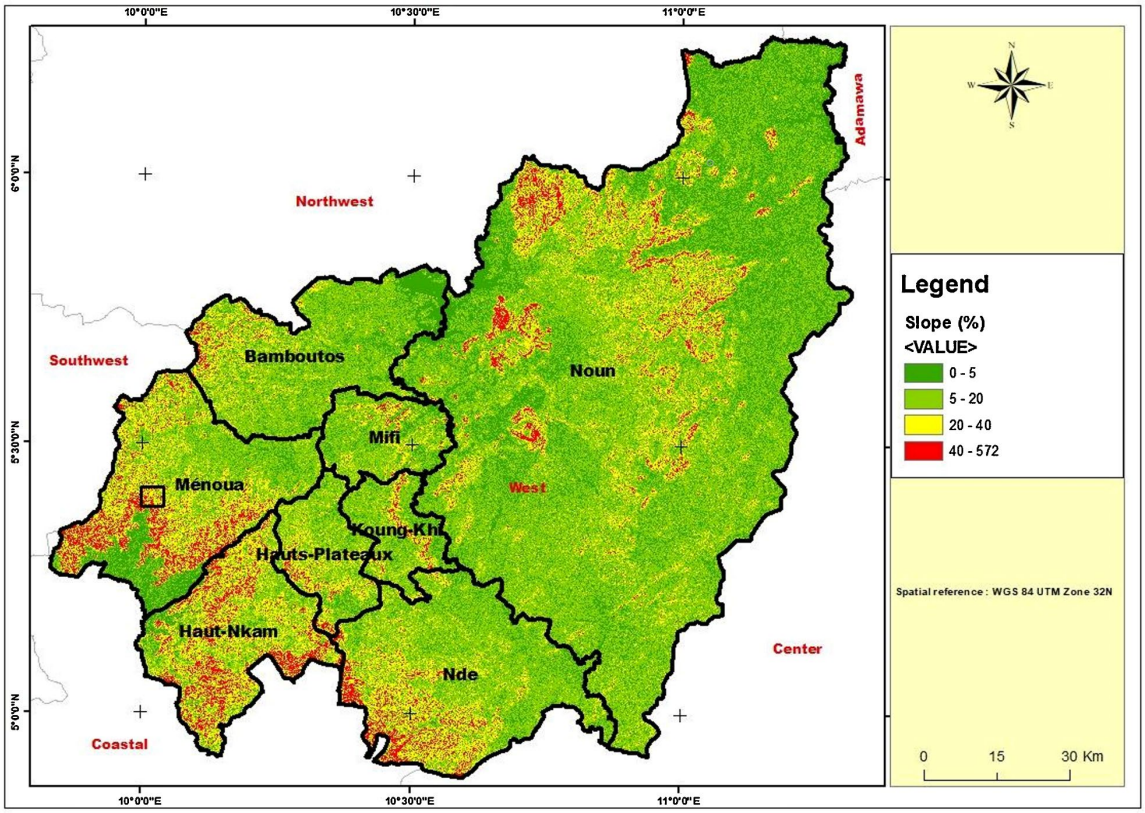
10°0'0"E
10°30'0"E
11°0'0"E
N.o.0.9
N.o.30.9
N.o.0.5
Adamawa
Northwest
Southwest
Bamboutos
Noun
Mifi
Ménoua
West
Koung-Khi
Hauts-Plateaux
Haut-Nkam
Nde
Center
Coastal
Legend
Slope (%)
<VALUE>
0 - 5
5 - 20
20 - 40
40 - 572
Spatial reference : WGS 84 UTM Zone 32N
0
15
30 Km

(a)

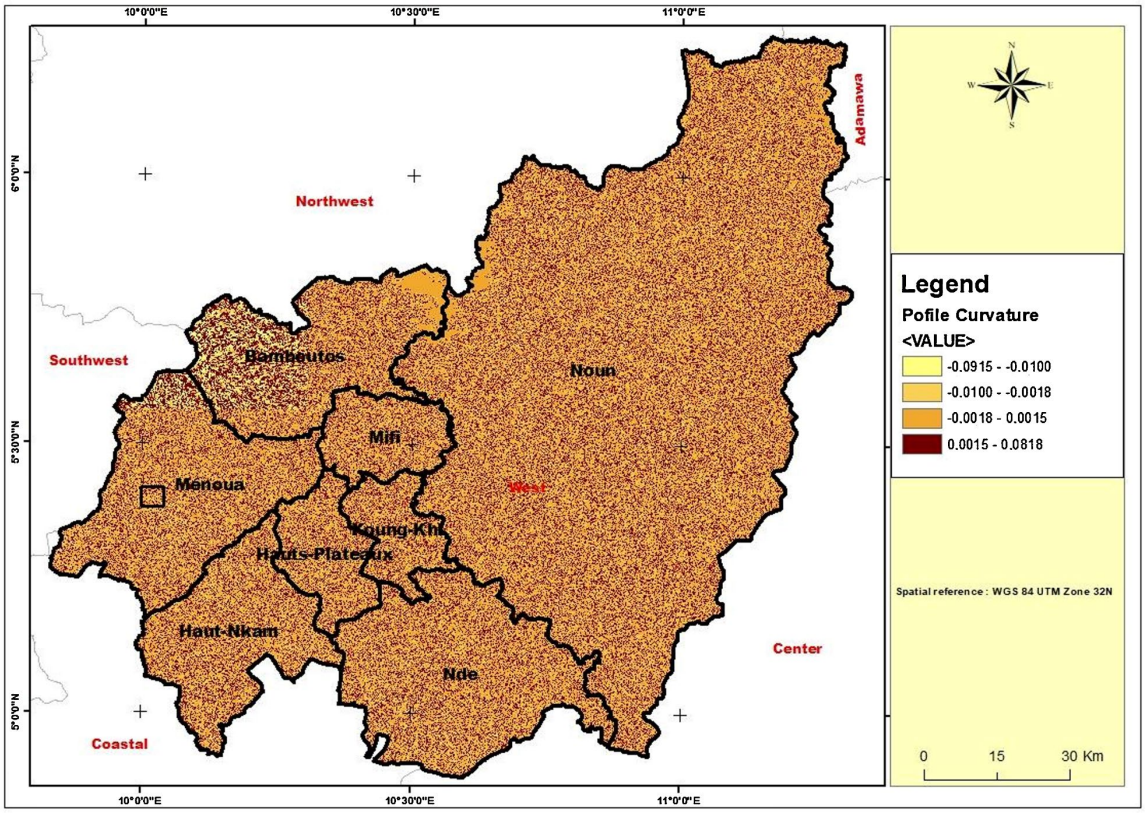
10°0'0"E
10°30'0"E
11°0'0"E
N.o.0.9
N.o.30.9
N.o.0.5
Adamawa
Northwest
Southwest
Bamboutos
Noun
Mifi
Ménoua
West
Koung-Khi
Hauts-Plateaux
Haut-Nkam
Nde
Center
Coastal
Legend
Pofile Curvature
<VALUE>
-0.0915 - -0.0100
-0.0100 - -0.0018
-0.0018 - 0.0015
0.0015 - 0.0818
Spatial reference : WGS 84 UTM Zone 32N
0
15
30 Km

(b)

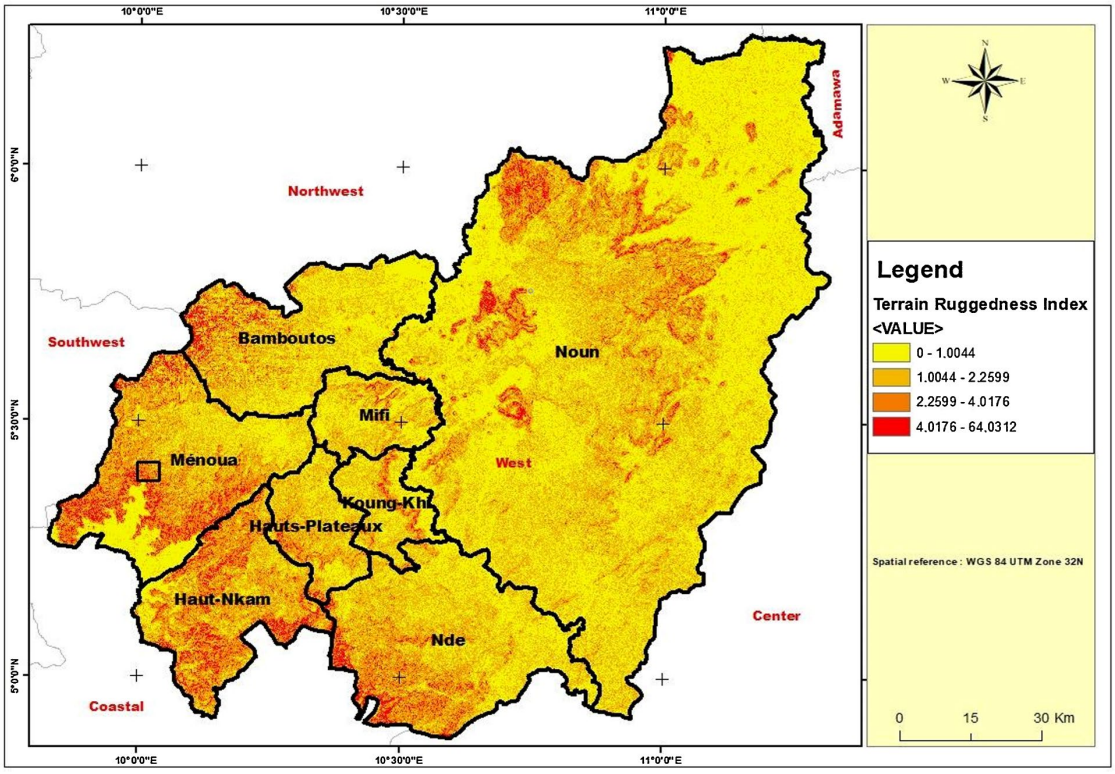

(c)

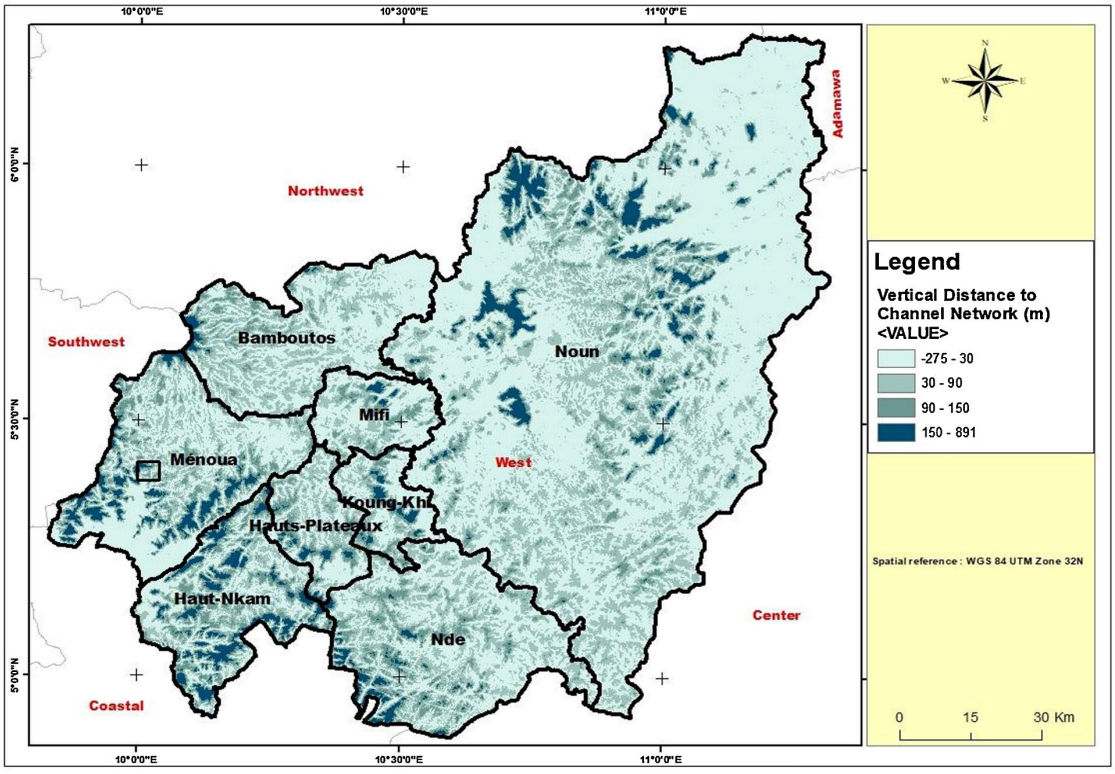

(d)

Figure 6. (a) Slope; (b) Profile of curvature; (c) Terrain ruggedness; (d) Terrain ruggedness. (Source: ArcGIS 10.8 (ESRI) software, from the topographic base sheets of Cameroon produced by the National Institute of Cartography).

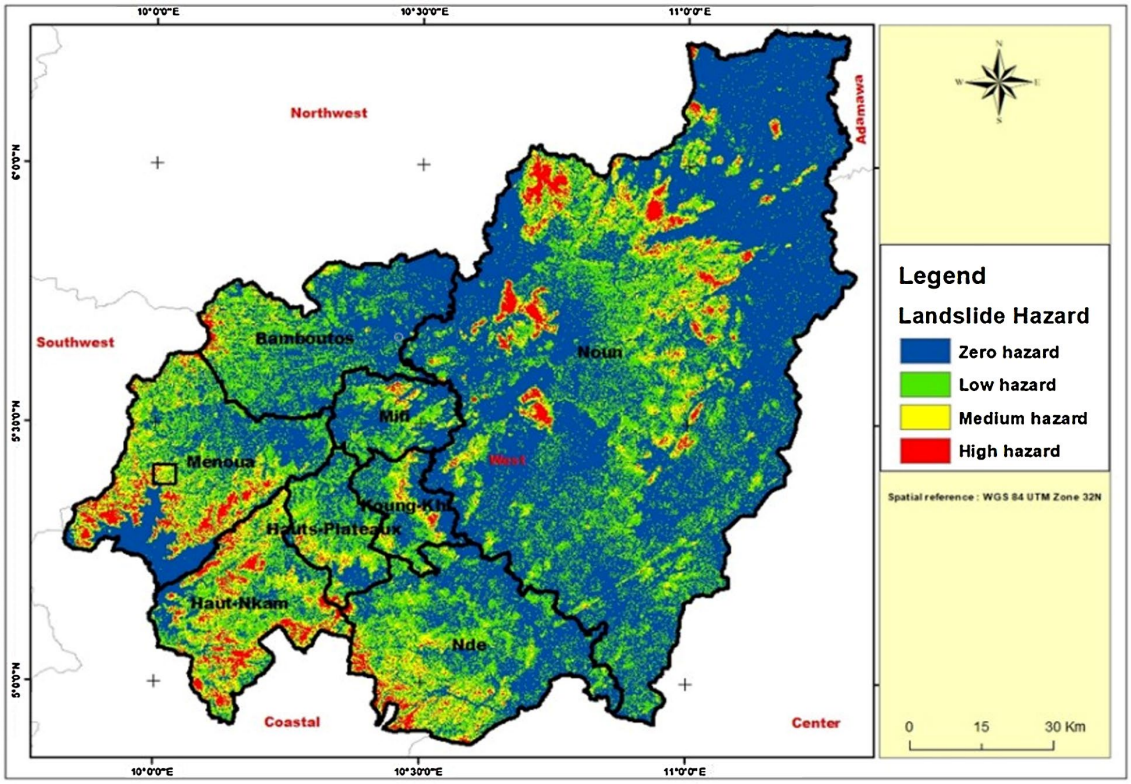

Figure 7. Risk map along the Foréké escarpement. (Source: ArcGIS 10.8 (ESRI) software, from the topographic base sheets of Cameroon produced by the National Institute of Cartography).

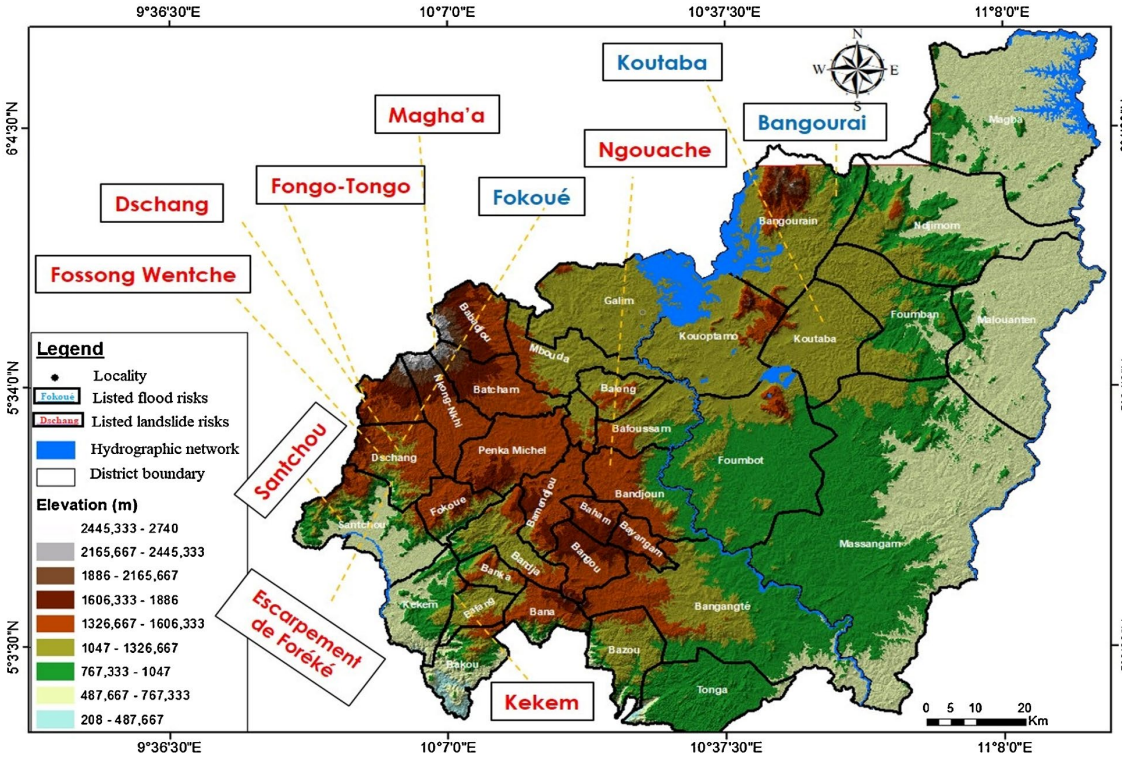

Figure 8. Past landslides map in the West Cameroon region. (Source: ArcGIS 10.8 (ESRI) software, from the topographic base sheets of Cameroon produced by the National Institute of Cartography).

5. Discussion

5.1. Choice of Method

Hazard defines natural conditions that combine to create a danger [35]-[37]. The hazard map is produced using Saaty's statistical spatial analysis model. In the literature, the selection of distribution center locations is based on multi-objective decision support metaheuristics (MMODM), multi-objective combinatorial optimization methods (MMOCO) and Multi-Criteria Decision support Methods (MCDM) [38]. MMODM methods optimize the situation after converting it into a single-objective problem, but they are very costly [39]. MMOCO methods solve discrete multicriteria problems for which the alternatives are not explicitly known [40]. The MCDM method evaluates alternatives and scenarios in order to select the most appropriate choice according to the objectives and results sought [41]. They fall into two categories, namely Multi-Objective Decision Support Methods (MODM) and Multi-Attribute Decision Support Methods (MADM). Unlike MADM, MODMs do not include quantitative criteria in the decision-making process [42]. However, for MADM, several approaches are not suitable for mapping natural hazards. For example, the Weight Sum Method (WSM) is recommended for one-dimensional problems, the Weighted Product Method (WPM) is dimensionless, and the TOPSIS technique (Technique for Order of Preference by Ideal Solution Similarity) is only suitable for decision-making for certain criteria [43]. ELECTRE multi-criteria methods take into account quantitative and qualitative criteria, the importance of criteria, and validate the solutions retained by simultaneous tests of agreement and disagreement, but they do not take into account interactions between criteria [44].

To overcome these limitations and meet the requirements of landslide hazard mapping in humid tropical mountain areas, we opted for Thomas Saaty's hierarchical multicriteria analysis method. Based on the comparison of pairs of options and criteria, it offers the advantages of hierarchical structuring (classes—criteria—weights), priority structuring (sub-criteria—ranks), and logical consistency [45]. It therefore leads to a justified choice, and the decision is then said to be rational, systematic and correctly made [46]. In terms of combining variables and formalizing expert rules, this method is the most comprehensive [47]-[50]. It retains the flexibility of the geomorphological approach while being more objective [51] [52]. It is widely used because of its generalizability and reproducibility [25] [53]. Previous landslides served as the basis for validation of the hazard map for the West Cameroon region. This field validation means that the model can be considered reliable [54] [55]. An inventory of past events is a prerequisite for any hazard assessment, whatever the scale of analysis and approach adopted [56] [57]. This is the principle of cross-validation, which uses non-overlapping spatial subsets of the mapped landslide to assess the accuracy of the prediction.

5.2. Choice of Input Parameters

Availability of high-resolution DTMs offers landslide cartographers the possibility

of accurately detecting landslide-prone areas [55] [58]. DEM enables precise visual analyses or automatic processing to facilitate certain geomorphological interpretations. In landslide studies, weightings can be transposed from one site to another if the geomorphological context is similar and if the input data are exactly the same in terms of resolution and variable classes [59]. Based on the natural factors predisposing to landslides on the Foréké escarpment, slope appears as the most important because it influences from 44% to 77% of landslides in humid tropical mountainous regions [60]. Soil loss increases exponentially with slope steepness [61]. Profile curvature is the second important factor, expressing the rate of change of the slope gradient and variations in flow velocity along the slope. A negative value signifies the surface is upwardly convex, while a positive value indicates it is upwardly concave, and a value of zero means the surface is linear [62]. On the Foréké escarpment, it varies between −0.03 and +0.03, characteristic of rugged relief [63]. According to [61], a convex slope tends to concentrate rainwater and runoff at its top, increasing the speed and volume of water and promoting the transport of materials, while a concave slope reduces material transport [63]. Terrain ruggedness index is the third factor. It measures the topographical complexity and increases as the terrain becomes more rugged, as observed on the study site. The altitude above the canal is the last factor. The higher altitude increases the force of gravity acting on the ground, increasing the risk of landslides.

5.3. The Double Landslide on Foréké Escarpment

The 15 km Santchou_Dschang road has a vertical drop of 737 m. The double landslide is the result of an imbalance created by the construction of a road on this very hilly site [64]-[68]. It has been demonstrated that, in the case of low mobilizable shear strength [69]-[72], several landslides can occur on the same site in clay soil [73] [74]. This finding is supported by the clay content, which varies between 69.35 and 82.69% in Foréké soils. On similar soils in the nearby locality of Kékem, [12] describe a very clayey material with high porosity (>29%), low cohesion (<0.5 bar) and a high angle of friction (15˚ - 22˚). The high clay content therefore significantly influenced the residual friction angle by decreasing the residual strength of the soils [75]-[77]. Creep movements have thus evolved into progressive landslides [74] [78]. This process is exacerbated by water infiltration, which accelerates the reduction in shear strength [79] due to the seasonal transition of the soil from a compact to a plastic state [80]. As a result, microcracks opened up in the clay material, altering cohesion [12] [64] and accelerating a landslide by creep. The impact of runoff is amplified by deforestation, which reduces rainwater infiltration [75]-[77] [81]. It should be noted that the conditions that prevailed at the end of the first landslide still prevail at the end of the second landslide, and further landslides are likely to occur on this hill (**Figure 9**).

5.3.1. Anthropogenic Constraints

The traffic on Dschang_Santchou is heavy, and the low speed of machinery impacts the amplitude of vibrations. These vibrations, caused in particular by trucks,

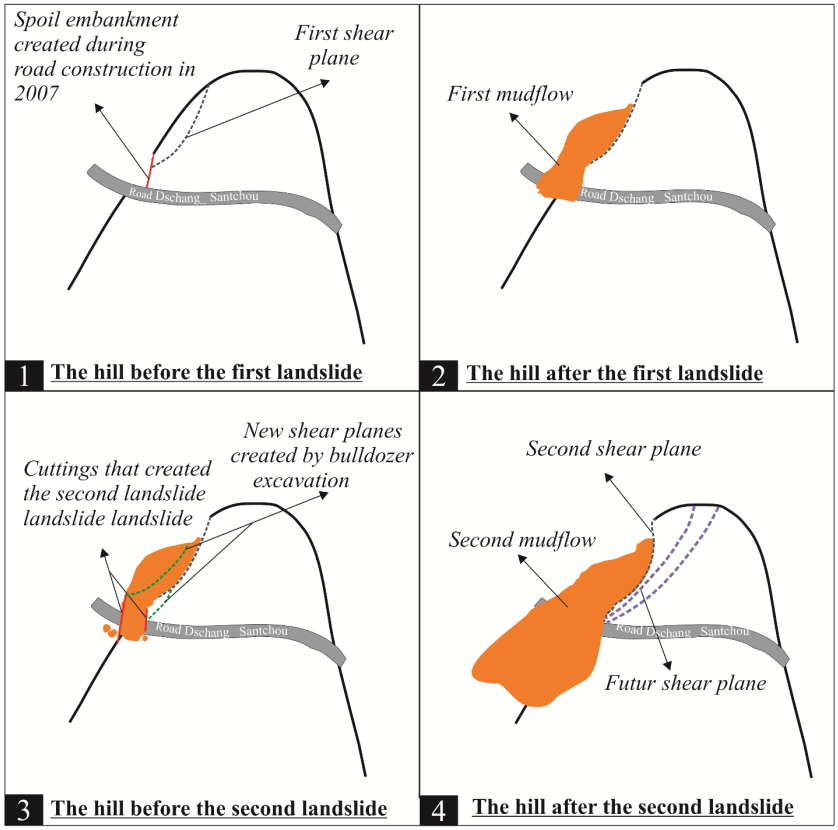

Figure 9. Schematic diagram of the process that led to the double landslide on the Foréké escarpment.

give rise to stress waves that propagate through the ground [82]. In addition, during construction of the P17 road, unsterilized cuttings embankments were built at mid-slope on very steep hillsides. [83] note that in such cases, due to slow and complex variations in interstitial overpressure, the most critical stability conditions may only appear in the long term. Indeed, the stiffening of the slope by the excavated material on its flank contributes significantly to increasing driving forces [84]. The second landslide, which occurred a few hours after the first, is a perfect illustration of anthropogenic action in triggering disasters [85] [86].

5.3.2. Natural Constraints

Landslides are very common in mountainous areas [37] [87] [88], on hills [12] [21] and along the high coasts [89]. The West Cameroon region is naturally predisposed to landslide risk due to its very rugged relief [27], the nature of its soils and its high rainfall [26]. The plains are linked to the plateau by escarpments [31] [33] such as Kékem and Foréké [12] [32], on which very clayey soils have developed [90] [91]. The CU triaxial shear performed by [12] on similar soils in the near locality of Kékem shows variations between 4 and 12 for apparent internal friction angle (φcu), 15 and 22 for effective internal friction angle (φ'cu), 0.15 and 0.50 bar for apparent cohesion (Ccu) and 0.10 and 0.38 bar for effective cohesion (C'cu). With low cohesion and a high angle of internal friction, the geotechnical

characteristics are unfavorable. Similarly, in the Kekem locality, [12] shows that the soil is saturated with water (80%), taking the material beyond the Atterberg limits (Wp = 28% - 39% and Wi = 52% - 81%).

5.3.3. Mitigation of Landslide Risk in the West Cameroon Region

In the West Cameroon region, landslides generally occur in July, August and September [28]. For the landslide of August 26, 1978, at Santchou, out of a total of 389 mm of water recorded during the month of August 1978, 88 mm of water were recorded on August 25, 1978, and 71 mm on August 26, 1978 [17]. Similar observations were made during the July 20, 2003 disaster in the Bambouto massif, where for a monthly average of 280 mm of water in July 2003, 84 mm of water were recorded during the two days preceding the landslide [19]. More recently, in the town of Bafoussam, 250 mm of rain fell continuously during the two days preceding the landslide on October 28, 2019 [92]. Monitoring rainfall data will alert people to potential landslide risks, and closing the Dschang-Santchou road to traffic during critical periods would be a good mitigation measure. In addition, to prevent landslides along the Dschang-Santchou line, all embankments over 2 meters high with a slope greater than 40% must be stabilized, as recommended by [93]. Combating creep landslides requires a comprehensive approach combining prevention and ground stabilization measures. Regular monitoring helps to anticipate landslides and assess the danger. Retaining walls or the insertion of steel bars in the ground are recommended along road embankments. The installation of drain sub-drains is necessary to evacuate water from the ground. Revegetation of embankments with deep-rooted plants is recommended to stabilize the soil and reduce water erosion. In the West Cameroon highlands, it is essential to carry out geotechnical studies before building any structures.

6. Conclusion

The West Cameroon region is naturally predisposed to landslide risk due to its very rugged relief, nature of soils and high rainfall. High-hazard zones represent 6.40% of the region. The double creep landslide of November 5, 2024, on the Foréké escarpment resulted from a combination of anthropogenic and natural factors. The conditions that prevailed at the end of the second landslide persist, and further landslides are likely to occur at this site. With 35% of the Dschang_Santchou stretch of road in a very high-hazard zone, it is imperative to carry out geotechnical studies to identify the imbalance factors along this stretch of National Road 17. Combating creep landslides requires a comprehensive approach combining prevention and ground stabilization measures. In the meantime, analysis of rainfall data can help detect exceptional rainfall and alert the population to potential landslide risks.

Conflicts of Interest

The authors declare no conflicts of interest.

References

[1] FAO (2008) La dégradation des sols s'intensifie. Viale delle Terme di Caracalla.

[2] Guo, Z., Ferrer, J.V., Hürlimann, M., Medina, V., Puig-Polo, C., Yin, K., *et al.* (2023) Shallow Landslide Susceptibility Assessment under Future Climate and Land Cover Changes: A Case Study from Southwest China. *Geoscience Frontiers*, **14**, Article ID: 101542. https://doi.org/10.1016/j.gsf.2023.101542

[3] Ebert, C. (1982) Les Catastrophes naturelles et leurs effets sur les nations en développement. *Science et Société*, **32**, 103-111.

[4] Achu, A.L., Aju, C.D., Thomas, J., Raicy, M.C., Yunus, A.P., Gopinath, G., *et al.* (2025) Decoding the Dynamics of July 2024 Mundakkai-Chooralmala Landslide in Kerala (India): An Analysis of Formation Mechanisms, Impacts and Lessons Learned. *Landslides*, **22**, 1181-1197. https://doi.org/10.1007/s10346-024-02454-y

[5] Yunus, A.P., Sajinkumar, K.S., Gopinath, G., Subramanian, S.S., Kaushal, S., Thanveer, J., *et al.* (2025) Chronicle of Destruction: The Wayanad Landslide of July 30, 2024. *Landslides*, **22**, 1891-1908. https://doi.org/10.1007/s10346-025-02494-y

[6] Gutiérrez, F., Soldati, M., Audemard, F. and Bălteanu, D. (2010) Recent Advances in Landslide Investigation: Issues and Perspectives. *Geomorphology*, **124**, 95-101. https://doi.org/10.1016/j.geomorph.2010.10.020

[7] Westerberg, C. (1998) Landslides in East African Highlands: Slope Instability and Its Interrelations with Landscape Characteristics and Land Use. *Advances in GeoEcology*, **31**, 325.

[8] Blais-Steven, A. (2020) Glissement de terrains historiques ayant causé des décès au Canada (1771-2019). Commission géologique du Canada. Ressources naturelles Canada.

[9] FAO (2017) Evaluation of Certain Contaminants in Food. 182.

[10] Segalen, P. (1967) Les sols et la géomorphologie du Cameroun. ORSTOM, 46.

[11] Leumbe, O. (2008) Evaluation et cartographie au moyen d'un système d'information géographique des zones à risques d'érosion et de glissement de terrain en région de montagne tropicale humide (mont Bambouto-Ouest Cameroun). Thèse Doctorat, Université de Yaoundé 1, 153.

[12] Aboubakar, B., Kagou, D., Guimolaire, N. and Ngapgue F. (2013) Instabilités de terrain dans les hautes terres de l'Ouest Cameroun: Caractérisation géologique et géotechnique du glissement de terrain de Kekem. *Bulletin de l'Institut Scientifique, Rabat, Section Sciences de la Terre*, No. 35, 39-51.

[13] Ferrer, J.V., Samprogna Mohor, G., Dewitte, O., Pánek, T., Reyes-Carmona, C., Handwerger, A.L., *et al.* (2024) Human Settlement Pressure Drives Slow-Moving Landslide Exposure. *Earth's Future*, **12**, e2024EF004830. https://doi.org/10.1029/2024ef004830

[14] Aboubakar, B. (2010) Etude géologique et géotechnique des mouvements de masse dans les hautes terres de l'ouest Cameroun: Cas des sites de Lepoh et Nteingue (Département de la Menoua) et de Kekem (Département du Haut-Nkam). Mémoire. Master Univetsity Dschang, 103 p.

[15] Puissant, A., Van Den Eeckhaut, M., Malet, J. and Maquaire, O. (2013) Landslide Consequence Analysis: A Region-Scale Indicator-Based Methodology. *Landslides*, **11**, 843-858. https://doi.org/10.1007/s10346-013-0429-x

[16] D.P.C. (2008) Rapport sur l'état de la protection civile au Cameroun. Direction de la protection civile du Cameroun, 305.

[17] Tchoua, F. (1984) Les coulées boueuses de Dschang (Août 1978). *Revue de géographie du Cameroun*, **4**, 25-33.

[18] Ayonghe, S.N., Ntasin, E.B., Samalang, P. and Suh, C.E. (2004) The June 27, 2001 Landslide on Volcanic Cones in Limbe, Mount Cameroon, West Africa. *Journal of African Earth Sciences*, **39**, 435-439. https://doi.org/10.1016/j.jafrearsci.2004.07.022

[19] Zogning, A. (2003) La catastrophe du 20 juillet 2003 à Magha'a. Rapport de terrain, 64.

[20] van Westen, C.J., van Asch, T.W.J. and Soeters, R. (2005) Landslide Hazard and Risk Zonation—Why Is It Still So Difficult? *Bulletin of Engineering Geology and the Environment*, **65**, 167-184. https://doi.org/10.1007/s10064-005-0023-0

[21] Broeckx, J., Rossi, M., Lijnen, K., Campforts, B., Poesen, J. and Vanmaercke, M. (2020) Landslide Mobilization Rates: A Global Analysis and Model. *Earth-Science Reviews*, **201**, Article ID: 102972. https://doi.org/10.1016/j.earscirev.2019.102972

[22] Bhuyan, K., Rana, K., Ferrer, J.V., Cotton, F., Ozturk, U., Catani, F., *et al.* (2024) Landslide Topology Uncovers Failure Movements. *Nature Communications*, **15**, Article No. 2633. https://doi.org/10.1038/s41467-024-46741-7

[23] Felsberg, A., Poesen, J., Bechtold, M., Vanmaercke, M. and De Lannoy, G.J.M. (2022) Estimating Global Landslide Susceptibility and Its Uncertainty through Ensemble Modeling. *Natural Hazards and Earth System Sciences*, **22**, 3063-3082. https://doi.org/10.5194/nhess-22-3063-2022

[24] Guzzetti, F., Carrara, A., Cardinali, M. and Reichenbach, P. (1999) Landslide Hazard Evaluation: A Review of Current Techniques and Their Application in a Multi-Scale Study, Central Italy. *Geomorphology*, **31**, 181-216. https://doi.org/10.1016/s0169-555x(99)00078-1

[25] Fell, R., Corominas, J., Bonnard, C., Cascini, L., Leroi, E. and Savage, W.Z. (2008) Guidelines for Landslide Susceptibility, Hazard and Risk Zoning for Land Use Planning. *Engineering Geology*, **102**, 85-98. https://doi.org/10.1016/j.enggeo.2008.03.022

[26] Njiosseu, E. (1998) Potentiels hydrologique du bassin versant de la Ménoua, flanc Sud-Ouest des monts Bambouto. Mémoire Maitrise en Sciences de la Terre, Université de Dschang, 50.

[27] Valet, S. (1985) Notices explicatives des cartes du climat, des paysages agro géologiques et des propositions d'aptitude à la mise en valeur des paysages agro géologiques de l'Ouest Cameroun au 1/200.000. CIRAT-IRAT, 120.

[28] Ngoufo, R. (1988) Les monts Bambouto, environnement et utilisation de l'espace. Thèse de Doctorat de 3ème cycle, Université de Yaoundé, 671.

[29] Tsalefack, M. (1999) Variation climatique, crise économique et dynamique des milieux agraires sur les Hautes Terres de l'Ouest. Thèse Doctorat d'Etat, Université de Yaoundé 1, 515.

[30] Schnell (1977) Introduction à la phytogéographie des pays tropicaux. Tome IV. La flore et la végétation de l'Afrique tropicale. Gauthier-Villars, 378.

[31] Olivry, J. (1986) Fleuves et Rivières du Cameroun. Collection monographie du Cameroun. 9th Edition, MESRES-ORSTOM, 733.

[32] Nyobe, J. (1987) A Geological and Geochemical Study of Fongo-Tongo and a Really Related Bauxite Deposits, Western Highlands, Republic of Cameroon. Thèse de Doctorat, University of Yaoundé, 287.

[33] Youmen, D. (1994) Evolution volcanique, pétrographique et temporelle de la caldeira des monts Bambouto (Cameroun). Thèse Doctorak, Université de Kiel, 273.

[34] Leumbe, O., Bitom, D., Tematio, P., Temgoua, E. and Lucas, Y. (2006) Etude des sols

ferralitiques à caractères andiques sur trachytes en zone de montagne humide tropicale (Mont Bambouto-Ouest Cameroun). *Etude et Gestion des Sols*, **12**, 313-326.

[35] Abbasi, I.A., Khan, M.A., Hadi, S., Ishfaq, M. and Mool, P. (2001) Geological Controls in Slope Failure and Landslide Hazards, Main Boundary Thrust Zone, Murree Hills, North Pakistan. *Journal of Asian Earth Sciences*, **19**, 3A, 1.

[36] Guzzetti, F., Mondini, A.C., Cardinali, M., Fiorucci, F., Santangelo, M. and Chang, K. (2012) Landslide Inventory Maps: New Tools for an Old Problem. *Earth-Science Reviews*, **112**, 42-66. https://doi.org/10.1016/j.earscirev.2012.02.001

[37] Leumbe, O., Bitom, Dieudonné., Mamdem L., Tiki, D. and Ibrahim, A. (2015) Cartographie des zones à risque d'inondation en zone Soudano-Sahélienne: Cas de Maga et ses environs dans la région de l'Extrême-Nord Cameroun. Afrique Science, 17.

[38] Agrebi, M., Abed, M. and Omri, M.N. (2017) ELECTRE I Based Relevance Decision-Makers Feedback to the Location Selection of Distribution Centers. *Journal of Advanced Transportation*, **2017**, Article ID: 7131094. https://doi.org/10.1155/2017/7131094

[39] Wolf, G.W. (2011) Facility Location: Concepts, Models, Algorithms and Case Studies. Series: Contributions to Management Science. *International Journal of Geographical Information Science*, **25**, 331-333. https://doi.org/10.1080/13658816.2010.528422

[40] Ashayeri, J. and Rongen, J.M.J. (1997) Central Distribution in Europe: A Multi-Criteria Approach to Location Selection. *The International Journal of Logistics Management*, **8**, 97-109. https://doi.org/10.1108/09574099710805628

[41] Sanayei, A., Farid Mousavi, S. and Yazdankhah, A. (2010) Group Decision Making Process for Supplier Selection with VIKOR under Fuzzy Environment. *Expert Systems with Applications*, **37**, 24-30. https://doi.org/10.1016/j.eswa.2009.04.063

[42] Zandi, A. and Roghanian, E. (2013) Extension of Fuzzy ELECTRE Based on VIKOR Method. *Computers & Industrial Engineering*, **66**, 258-263. https://doi.org/10.1016/j.cie.2013.06.011

[43] Hu, H., Kandampully, J. and Juwaheer, T.D. (2009) Relationships and Impacts of Service Quality, Perceived Value, Customer Satisfaction, and Image: An Empirical Study. *The Service Industries Journal*, **29**, 111-125. https://doi.org/10.1080/02642060802292932

[44] Mena, B. (2000) Introduction aux méthodes multicritères d'aide à la décision. *Biotechnology*, *Agronomy*, *Society and Environment*, **4**, 83-93.

[45] Skibniewski, M.J. and Chao, L. (1992) Evaluation of Advanced Construction Technology with AHP Method. *Journal of Construction Engineering and Management*, **118**, 577-593. https://doi.org/10.1061/(asce)0733-9364(1992)118:3(577)

[46] Al-Harbi, K.M.A. (2001) Application of the AHP in Project Management. *International Journal of Project Management*, **19**, 19-27. https://doi.org/10.1016/s0263-7863(99)00038-1

[47] Thiery, Y., Malet, J., Sterlacchini, S., Puissant, A. and Maquaire, O. (2005) Analyse spatiale de la susceptibilité des versants aux glissements de terrains. Comparaison de deux approches spatialisées par SIG. *Revue Internationale de Géomatique*, **15**, 227-245. https://doi.org/10.3166/rig.15.227-245

[48] Fressard, M., Thiery, Y. and Maquaire, O. (2014) Which Data for Quantitative Landslide Susceptibility Mapping at Operational Scale? Case Study of the Pays D'auge Plateau Hillslopes (Normandy, France). *Natural Hazards and Earth System Sciences*, **14**, 569-588. https://doi.org/10.5194/nhess-14-569-2014

[49] Corominas, J., van Westen, C., Frattini, P., Cascini, L., Malet, J., Fotopoulou, S., *et al.*

(2013) Recommendations for the Quantitative Analysis of Landslide Risk. *Bulletin of Engineering Geology and the Environment*, **73**, 209-263. https://doi.org/10.1007/s10064-013-0538-8

[50] Reichenbach, P., Rossi, M., Malamud, B.D., Mihir, M. and Guzzetti, F. (2018) A Review of Statistically-Based Landslide Susceptibility Models. *Earth-Science Reviews*, **180**, 60-91. https://doi.org/10.1016/j.earscirev.2018.03.001

[51] Poiraud, A. (2014) Landslide Susceptibility-Certainty Mapping by a Multi-Method Approach: A Case Study in the Tertiary Basin of Puy-en-Velay (Massif Central, France). *Geomorphology*, **216**, 208-224. https://doi.org/10.1016/j.geomorph.2014.04.001

[52] Nanfack, G. and Julius, T. (2020) Cartographie de susceptibilité au glissement de terrain dans le bassin versant de la Menoua (Ouest-Cameroun) au moyen de l'Analyse Multicritère Hiérarchique. *Revue International de géomatique, Aménagement et Gestion des Ressources*, **7**, 59-73.

[53] Thiery, Y., Reninger, P., Lacquement, F., Raingeard, A., Lombard, M. and Nachbaur, A. (2017) Analysis of Slope Sensitivity to Landslides by a Transdisciplinary Approach in the Framework of Future Development: The Case of La Trinité in Martinique (French West Indies). *Geosciences*, **7**, Article No. 135. https://doi.org/10.3390/geosciences7040135

[54] Van Den Eeckhaut, M., Reichenbach, P., Guzzetti, F., Rossi, M. and Poesen, J. (2009) Combined Landslide Inventory and Susceptibility Assessment Based on Different Mapping Units: An Example from the Flemish Ardennes, Belgium. *Natural Hazards and Earth System Sciences*, **9**, 507-521. https://doi.org/10.5194/nhess-9-507-2009

[55] Guzzetti, F., Carrara, A., Cardinali, M. and Reichenbach, P. (1999) Landslide Hazard Evaluation: A Review of Current Techniques and Their Application in a Multi-Scale Study, Central Italy. *Geomorphology*, **31**, 181-216. https://doi.org/10.1016/s0169-555x(99)00078-1

[56] Remondo, J., González-Díez, A., De Terán, J.R.D. and Cendrero, A. (2003) Landslide Susceptibility Models Utilising Spatial Data Analysis Techniques. a Case Study from the Lower Deba Valley, Guipuzcoa (Spain). *Natural Hazards*, **30**, 267-279. https://doi.org/10.1023/b:nhaz.0000007202.12543.3a

[57] Chung, C. and Fabbri, A.G. (2008) Predicting Landslides for Risk Analysis—Spatial Models Tested by a Cross-Validation Technique. *Geomorphology*, **94**, 438-452. https://doi.org/10.1016/j.geomorph.2006.12.036

[58] Eeckhaut, M.V.D., Poesen, J., Verstraeten, G., Vanacker, V., Nyssen, J., Moeyersons, J., *et al.* (2006) Use of LIDAR-Derived Images for Mapping Old Landslides under Forest. *Earth Surface Processes and Landforms*, **32**, 754-769. https://doi.org/10.1002/esp.1417

[59] Thiery, Y., Lacquement, F. and Marçot, N. (2019) Landslides Triggered in Weathered Crystalline Rocks of Moderate Latitudes: A Case Study in Mediterranean Environment (the Maures Massif, France). *Engineering Geology*, **248**, 164-184. https://doi.org/10.1016/j.enggeo.2018.12.002

[60] Rice, R.M. and Foggin, G.T. (1971) Effect High Intensity Storms on Soil Slippage on Mountainous Watersheds in Southern California. *Water Resources Research*, **7**, 1485-1496. https://doi.org/10.1029/wr007i006p01485

[61] Roose, E. (1981) Dynamique actuelle des sols ferrallitiques et ferrugineux tropicaux d'Afrique occidentale. Etude expérimentale des transferts hydrologiques et biologiques des matières sous végétations naturelles ou cultivés. Thèse Doct. ès Sci-ences, Univers. d'Orléans, Travaux et Documents ORSTOM, 130, 569.

[62] Farin, G. (2016) Curvature Combs and Curvature Plots. *Computer-Aided Design*, **80**,

6-8. https://doi.org/10.1016/j.cad.2016.08.003

[63] Qiu, S., Hou, Y. and Ming, H.X.G. (2018) An Implicit Method for Probabilistic Common-Cause Failure Analysis Using Bayesian Network. *IFAC-PapersOnLine*, **51**, 1037-1042. https://doi.org/10.1016/j.ifacol.2018.09.718

[64] Blondeau, F. and Josseaume H. (1976) Mesure de la résistance au cisaillement résiduelle en laboratoire. *Bulletin de liaison des laboratoires des ponts et chaussées*, *stabilité des talus*, *versants naturels*, *Numéro spécial II*, **1976**, 90-106.

[65] Westerberg and Christiansson, C. (1998) Landslides in East African Highlands: Slope Instability and Its Interrelations with Landscape Characteristics and Land Use. *Advances in GeoEcology*, **31**, 317-325.

[66] Bogdan, M., Savulescu, I., Sandric and Razvan, O. (2006) Application de la détection des changements à l'étude de la dynamique de la végétation des Monts de Bucegi (Carpates Méridionales, Roumanie). *Télédétection*, **6**, 215-231.

[67] Blondeau, F., Blivet, J. and Ung Seng, V. (1976) Résistance au cisaillement des argiles raides. *Bulletin des Laboratoires des Ponts et Chaussées*, n˚ spécial III "Déblais et remblais", 23-38.

[68] Hawkins, A. and Privett, K. (1985) Discussion on the Residual Shear Strength of Cohesive Soils. *Ground Engin*eering, **18**, 22-29.

[69] Felix, B. (1980) Le fluage des sols argileux, étude bibliographique. Rapport de Recherche L. P. C., 93, 234.

[70] Silleran, A. (1981) Glissements de terrain liés à des travaux. *Revue Française de Géotechnique*, No. 14, 198-202. https://doi.org/10.1051/geotech/198114b198

[71] Crozier, M.J. (2005) Multiple-Occurrence Regional Landslide Events in New Zealand: Hazard Management Issues. *Landslides*, **2**, 247-256. https://doi.org/10.1007/s10346-005-0019-7

[72] Alvioli, M., Marchesini, I., Reichenbach, P., Rossi, M., Ardizzone, F., Fiorucci, F., *et al*. (2016) Automatic Delineation of Geomorphological Slope Units with r.slopeunits V1.0 and Their Optimization for Landslide Susceptibility Modeling. *Geoscientific Model Development*, **9**, 3975-3991. https://doi.org/10.5194/gmd-9-3975-2016

[73] Gosset, J. and Khizardjian J. (1976) Étude de la tranchée d'essai du Tronchon sur l'autoroute A6. *Bulletin des Laboratoires des Ponts et Chaussées*, n˚ spécial III "Déblais et remblais", 49-58.

[74] Flotte, J.P. (1981) Mouvements liés à des travaux de défense et de restauration des sols. *Revue Française de Géotechnique*, No. 14, 194-197. https://doi.org/10.1051/geotech/198114b194

[75] Bollot, N., Devos, A. and Pierre, G. (2015) Ressources en eau et glissements de terrain: Exemple du bassin versant de la Semoigne (Bassin de Paris, France). *Géomorphologie*: *Relief*, *Processus*, *Environnement*, **21**, 7-20. https://doi.org/10.4000/geomorphologie.10826

[76] Capitani, C., van Soesbergen, A., Mukama, K., Malugu, I., Mbilinyi, B., Chamuya, N., *et al*. (2018) Scenarios of Land Use and Land Cover Change and Their Multiple Impacts on Natural Capital in Tanzania. *Environmental Conservation*, **46**, 17-24. https://doi.org/10.1017/s0376892918000255

[77] Mayne, P.W., Jones, J.S. and Dumas, J.C. (1984) Ground Response to Dynamic Compaction. *Journal of Geotechnical Engineering*, **110**, 757-774. https://doi.org/10.1061/(asce)0733-9410(1984)110:6(757)

[78] Magnan, J. (1979) Étude numérique de la consolidation unidimensionnelle en tenant compte des variations de la perméabilité et de la compressibilité du sol, du fluage et

de la non saturation. *Bulletin de liaison des Laboratoires des Ponts et Chaussées*, **103**, 83-94.

[79] Steger, S., Schmaltz, E. and Glade, T. (2020) The (F)utility to Account for Pre-Failure Topography in Data-Driven Landslide Susceptibility Modelling. *Geomorphology*, **354**, Article ID: 107041. https://doi.org/10.1016/j.geomorph.2020.107041

[80] Duchaufour, P. (1977) Pédologie: Pédogenèse et classification. Doc. 2ème Edition, Masson, 491.

[81] Kengni, L., Tekoudjou, H., Tematio, P., Pamo, Tedongkeng, E., Tankou, C., Lucas, Y. and Probst, J. (2009) Rainfall Variability along the Southern Flank of the Bambouto Mountain (West-Cameroon). *Journal of the Cameroon Academy of Sciences*, **8**, 45-52.

[82] Hunaidi, O. and Tremblay, M. (1997) Traffic-Induced Building Vibrations in Montréal. *Canadian Journal of Civil Engineering*, **24**, 736-753. https://doi.org/10.1139/l97-023

[83] Amar, S., Gaudin, B., Legrand, J. and Londez, M. (1973) Franchissement de zones instables par des voies autoroutieres. Comptes rendus. *Symposium* "*Sol et sous-sol. Sécurité des constructions*", Vol. 1, 247-271.

[84] Van Den Eeckhaut, M., Verstraeten, G. and Poesen, J. (2007) Morphology and Internal Structure of a Dormant Landslide in a Hilly Area: The Collinabos Landslide (Belgium). *Geomorphology*, **89**, 258-273. https://doi.org/10.1016/j.geomorph.2006.12.005

[85] Thiery, Y., Malet, J., Sterlacchini, S., Puissant, A. and Maquaire, O. (2007) Landslide Susceptibility Assessment by Bivariate Methods at Large Scales: Application to a Complex Mountainous Environment. *Geomorphology*, **92**, 38-59. https://doi.org/10.1016/j.geomorph.2007.02.020

[86] Regmi, N.R., Giardino, J.R. and Vitek, J.D. (2013) Characteristics of Landslides in Western Colorado, USA. *Landslides*, **11**, 589-603. https://doi.org/10.1007/s10346-013-0412-6

[87] Malik, M. and Farooq, S. (1996) Landslide Hazard Management and Control in Pakistan: A Review. ICIMOD, 68.

[88] Zangmo, G.T., Kagou, A.D., Nkouathio, D.G. and Wandji, P. (2009) Typology of Natural Hazards and Assessment of Associated Risks in the Mount Bambouto Caldera (Cameroon Line, West Cameroon). *Acta Geologica Sinica-English Edition*, **83**, 1008-1016. https://doi.org/10.1111/j.1755-6724.2009.00130.x

[89] Camilo, D.C., Lombardo, L., Mai, P.M., Dou, J. and Huser, R. (2017) Handling High Predictor Dimensionality in Slope-Unit-Based Landslide Susceptibility Models through Lasso-Penalized Generalized Linear Model. *Environmental Modelling & Software*, **97**, 145-156. https://doi.org/10.1016/j.envsoft.2017.08.003

[90] Tematio, P. and Olson, K.R. (1997) Impacts of Industrialized Agriculture on Land in Bafou, Cameroon. *Journal of Soil and Water Conservation*, **52**, 404-405. https://doi.org/10.1080/00224561.1997.12457180

[91] Leumbe, O.L., Bitom, D. and Assako, R.A. (2012) Évaluation des pertes en terres en région de montagne tropicale humide (cas du massif volcanique des Bambouto-Ouest Cameroun). In: *Lutte antiérosive, réhabilitation des sols tropicaux et protection contre les pluies exceptionnelles*, IRD Éditions, 530-540. https://doi.org/10.4000/books.irdeditions.13859

[92] Tangmouo, T., Yemmafouo, F. and Ngouanet C. (2020) Cartographie de la susceptibilité aux glissements de terrain à Bafoussam (Cameroun). Approche par analyse

multicritère hiérarchique et Système d'Information Géographique. *Revue Internationale de Géomatique*, *Aménagement et Gestion des Ressources*, **7**, 30.

[93] Wong, F.S. (1984) Uncertainties in FE Modeling of Slope Stability. *Computers & Structures*, **19**, 777-791. https://doi.org/10.1016/0045-7949(84)90177-9